

Enhancing Chemosensitivity in ABCB1- and ABCG2-Overexpressing Cells and Cancer Stem-like Cells by An Aurora Kinase Inhibitor CCT129202

Chao Cheng,^{*,†,‡} Zhen-guo Liu,^{†,‡} Hui Zhang,[§] Jing-dun Xie,[§] Xing-gui Chen,[§] Xiao-qin Zhao,[§] Fang Wang,[§] Yong-ju Liang,[§] Li-kun Chen,[§] Satyakam Singh,^{||} Jun-jiang Chen,^{||} Tanaji T. Talele,^{||} Zhe-sheng Chen,^{||} Fo-tian Zhong,[†] and Li-wu Fu^{*,§}

[†]Department of Thoracic Surgery, The First Affiliated Hospital of Sun Yat-Sen University, Guangzhou 510080, China

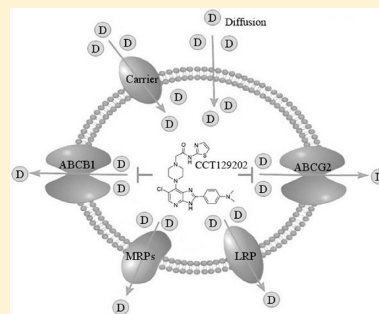
[§]State Key Laboratory of Oncology in South China, Cancer Center, Sun Yat-Sen University, Guangzhou 510060, China

^{||}Department of Pharmaceutical Sciences, College of Pharmacy and Allied Health Professions, St. John's University, Queens, New York 11439, United States

S Supporting Information

ABSTRACT: Imidazopyridine CCT129202 is an inhibitor of Aurora kinase activity and displays a favorable antineoplastic effect in preclinical studies. Here, we investigated the enhanced effect of CCT129202 on the cytotoxicity of chemotherapeutic drugs in multidrug resistant (MDR) cells with overexpression of ATP-binding cassette (ABC) transporters and cancer stem-like cells. CCT129202 of more than 90% cell survival concentration significantly enhanced the cytotoxicity of substrate drugs and increased the intracellular accumulations of doxorubicin and rhodamine 123 in ABCB1 and ABCG2 overexpressing cells, while no effect was found on parental sensitive cells. Interestingly, CCT129202 also potentiated the sensitivity of cancer stem-like cells to doxorubicin. Importantly, CCT129202 increased the inhibitory effect of vincristine and paclitaxel on ABCB1 overexpressing KBv200 cell xenografts in nude mice and human esophageal cancer tissue overexpressing ABCB1 *ex vivo*, respectively. Furthermore, the ATPase activity of ABCB1 was inhibited by CCT129202. Homology modeling predicted the binding conformation of CCT129202 within the large hydrophobic cavity of ABCB1. On the other hand, CCT129202 neither apparently altered the expression levels of ABCB1 and ABCG2 nor inhibited the activity of Aurora kinases in MDR cells under the concentration of reversal MDR. In conclusion, CCT129202 significantly reversed ABCB1- and ABCG2-mediated MDR *in vitro*, *in vivo* and *ex vivo* by inhibiting the function of their transporters and enhanced the eradication of cancer stem-like cells by chemotherapeutic agents. CCT129202 may be a candidate as MDR reversal agent for antineoplastic combination therapy and merits further clinical investigation.

KEYWORDS: CCT129202, multidrug resistance, ATP-binding cassette transporters, aurora kinase inhibitor, cancer stem-like cells



INTRODUCTION

Chemotherapy is a main treatment modality against cancer in the clinic. However, the clinical benefits of chemotherapy are quite often disappointing, and treatment failures are partly attributed to the overexpression of ATP-binding cassette (ABC) transporters.¹ The ABC transporters are a series of transmembrane proteins, which are able to extrude a broad range of functionally and structurally unrelated substrates out of cancer cells with the energy from ATP hydrolysis.² In the human genome, the ABC efflux transporter family has forty-nine members classified into seven subfamilies.³ Among them, P-glycoprotein (P-gp/ABCB1), the breast cancer resistance protein (BCRP/ABCG2), and the multidrug resistance protein 1 (MRP1/ABCC1) are particularly important due to their prevalence and roles in MDR.^{3,4}

The side population (SP) of cancer cells, which have a stem cell-like phenotype, are present in diverse tumor types; these stem-like cancer cells are resistant to chemotherapy partly due

to overexpression of ABC transporters such as ABCB1 and ABCG2. Relapse of cancer following conventional or targeted cancer therapy is likely due to surviving cancer stem-like cells, the eradication of which might cure the cancer.⁵ However, current therapeutic modalities may not effectively ablate the cancer stem-like cells; potentiation of the cytotoxicity of conventional chemotherapeutics to increase the eradication of cancer stem-like cells is one key strategy to cure cancer.⁶

In the past few years, the combination of targeted agents and traditional chemotherapeutics has gradually become a new strategy for the treatment of cancer patient. Lapatinib, a tyrosine kinase inhibitor of both EGFR and HER-2, revealed a reversal effect of MDR in *in vitro* and *in vivo* by inhibiting the

Received: December 29, 2011

Revised: May 1, 2012

Accepted: May 27, 2012

Published: May 27, 2012

function of ABCB1 and ABCG2, enhancing the cytotoxicity of their substrates, such as paclitaxel, vincristine, et al.⁷ In the clinical trials, in patients with HER-2 positive metastatic breast cancer, lapatinib plus paclitaxel treatment produced an encouraging overall response rate with manageable toxicities.⁸ These suggest that the combined therapy of small molecules that target the ATP-binding pocket of tyrosine kinases and conventional chemotherapeutic drugs may enhance the antitumor effectiveness by modulating MDR.

The Aurora kinase family belongs to a subfamily of serine/threonine kinases, which is essential for the regulation of centrosome maturation, mitotic spindle formation, chromosome segregation and cytokinesis during mitosis.^{9,10} The expression of Aurora-A and Aurora-B is elevated in a variety of human cancers and is associated with poor prognosis.^{11,12} The potential role of Aurora kinases in regulating cell mitosis and tumorigenesis makes them attractive targets for anticancer therapy. A series of Aurora kinase inhibitors have been developed and introduced into clinical trials, such as ZM447439, AZD-1152, PHA-680632 and MK-0457.¹³⁻¹⁶ Lin et al. currently reported that MK-0457 in combination with docetaxel significantly reduced tumor growth beyond docetaxel alone in a HeyA8-MDR model.¹⁷ Taken together, these discoveries suggest that Aurora kinase inhibitors appear to be promising inhibitors/modulators of not only mitosis but also MDR.

CCT129202 is a novel, small-molecule inhibitor with high selectivity against the Aurora kinase family but not other tyrosine kinases.⁹ It is an imidazole derivative with multiple amine groups in the chemical structure and is hydrophobic in nature; thus it possesses the structural characteristic of ABCB1 substrates and modulators.^{18,19} However, its affinity or effect on ABCs has not been evaluated. Taken together, these findings prompted us to evaluate whether CCT129202 could enhance the anticancer efficacy of traditional chemotherapeutics by interacting with ABC transporters *in vitro*, *in vivo* and *ex vivo*.

■ EXPERIMENTAL SECTION

Materials. CCT129202 was purchased from Selleck Chemicals. MTT, doxorubicin, rhodamine 123, vincristine, topotecan, paclitaxel, mitoxantrone, verapamil (VRP), fumitremorgin C (FTC), MK-571 sodium salt hydrate, Hoechst 33342 and other chemicals were obtained from Sigma Chemical Co. (St. Louis, MO). DMEM and RPMI 1640 were products of Gibco BRL (Gaithersburg, MD). Monoclonal antibodies against ABCB1 (sc-55510), ABCC1 (sc-18835), p21 and glyceraldehyde-3-phosphate dehydrogenase (GAPDH) were from Santa Cruz Biotechnology (Santa Cruz, CA); ABCG2 antibody (MAB4146) was obtained from Chemicon International, Inc. (Billerica, MA); antibodies against Aurora A and phospho-Aurora A (Thr288) were obtained from Cell Signaling Technology (Danvers, MA); monoclonal antibody against c-Myc was from BD Bioscience (San Jose, CA).

Cell Lines and Cell Culture. The following cell lines were cultured in DMEM or RPMI 1640 with 10% fetal bovine serum (FBS) at 37 °C in a humidified atmosphere of 5% CO₂: the human oral epidermoid carcinoma cell line KB and its vincristine-selected ABCB1-overexpressing derivative KBv200,²⁰ the human breast carcinoma cell line MCF-7 and its doxorubicin-selected ABCB1-overexpressing derivative MCF-7/adr;²¹ the human colon carcinoma cell line S1 and its mitoxantrone-selected ABCG2-overexpressing derivative S1-M1-80;²² the human leukemia cell lines HL60 and its

doxorubicin-selected ABCC1-overexpressing derivative HL60/adr; the lung cancer cell A549; the human primary embryonic kidney cell line HEK293 and its pcDNA3.1, ABCB1 and ABCG2 stable gene-transfected cell lines HEK293/pcDNA3.1, HEK293/ABCB1²³ and HEK293/ABCG2-T7.²² The transfected cells were cultured in DMEM with 2 mg/mL G418.

Cytotoxicity Assay. MTT assay was used to assess the antiproliferation activity.²⁴ The drug concentration resulting in 50% inhibition of cell growth (IC₅₀) was determined by the Bliss method.²⁵ The degree of resistance was estimated by dividing the IC₅₀ for the MDR cells by that of the parental sensitive cells; the fold-reversal factor of MDR was calculated by dividing the IC₅₀ of the anticancer drug in the absence of CCT129202 by the one obtained in the presence of CCT129202.

Doxorubicin and Rhodamine 123 Accumulation. The effect of CCT129202 on the intracellular accumulation of doxorubicin or rhodamine 123 was measured by flow cytometry as previously described.²¹ Verapamil, a known ABCB1 inhibitor, was used as a positive control in ABCB1 overexpressing cells; FTC, an ABCG2 specific inhibitor, was used as a positive control in overexpressing ABCG2 cells in accumulation assays.^{20,26}

Western Blot Analysis. Western blot was performed as previously described.²⁷ To determine whether CCT129202 affects the expression of ABCB1 and ABCG2, the cells were treated with different concentrations (0.125–2 μM) of CCT129202 for 48 h. To evaluate whether CCT129202, at reversal concentrations, is able to inhibit the Aurora kinase signaling pathway, cells were incubated with various concentrations of CCT129202 for 24 h.

Reverse Transcription PCR and Real-Time PCR. After drug treatment for 48 h, total cellular RNA was isolated by TRIzol Reagent RNA extraction kit (Molecular Research Center, Cincinnati, OH) following the manufacturer's instruction. The first strand cDNA was synthesized using Oligo dT primers with reverse transcriptase (Promega Corp., Madison, WI). PCR primers were 5'-ccatcattgcaatagcagg-3' (forward) and 5'-gttcaactctgctcctga-3' (reverse) for ABCB1; 5'-tgctgtcatggcttcagta-3' (forward) and 5'-gccactgattctccaca-3' (reverse) for ABCG2; 5'-cttggatctgtggaagga-3' (forward) and 5'-caccctgttgctgtagcc-3' (reverse) for GAPDH, respectively.²⁸ After 35 cycles of amplification, products were resolved and examined by 1.5% agarose gel electrophoresis.

Real-time PCR was performed on cDNA samples using an ABI PRISM 7500 Sequence Detection System (Applied Biosystems, Foster City, CA). Reactions were carried out at least in triplicate repeats in three independent experiments. Primers for ABCB1 were 5'-gtggggcaagtgcattcatt-3' (forward), 5'-tcttcacccaggctcagt-3' (reverse); primers for ABCG2 were 5'-cacctattggcctcaggaa-3' (forward), 5'-cctgcttgaaggctctatg-3' (reverse); primers for GAPDH were 5'-gagtaacggattgtgctg-3' (forward), 5'-gatctcgtcctggaagatg-3'.²⁹

Cell Cycle Analysis. Control and drug-treated cells were harvested, washed twice with ice-cold PBS, and fixed with 70% ethanol for 12 h or overnight at 4 °C. Cells were washed twice using ice-cold PBS, and then incubated with propidium iodide (50 μg/mL) and RNase (50 μg/mL) for 30 min at room temperature away from light. DNA content was analyzed by flow cytometry (Beckman Coulter, Cytomics FC500, Fullerton, CA).³⁰

ATPase Assay of ABCB1. The ATPase activity of verapamil-stimulated ABCB1 in the membrane vesicles of

High Five insect cells was measured by Pgp-Glo assay systems (Promega, Madison, WI) as previously described.²⁸ Various concentrations of CCT129202 were diluted and then incubated with 0.1 mM verapamil, 5 mM Mg-ATP and 25 μg of recombinant human ABCB1 membranes at 37 °C for 40 min. Luminescence was initiated by ATP detection buffer. After incubation at room temperature for another 20 min, the white opaque 96-well plate (Corning, Shanghai, China) was read on a luminometer (SpectraMax M5, Molecular Devices, Sunnyvale, CA). The changes of relative light units (ΔRLU) were measured by comparing Na_3VO_4 -treated samples with CCT129202 and verapamil combination-treated samples. The ATP consumed was obtained by comparing to a standard curve.

Patients and Tumor Histoculture End-Point Staining Computer Image Analysis (TECIA). The cohort consisted of 20 patients who were diagnosed with esophageal squamous carcinoma between March 2, 2011, and August 26, 2011, at the Department of Thoracic Surgery, the First Affiliated Hospital of Sun Yat-Sen University. The study was approved by the Committee for the Conduct of Human Research and Institutional Review Board of the First Affiliated Hospital of Sun Yat-Sen University, and informed consent was obtained from each patient.

TECIA is an improved histoculture drug response assay (HDRA) as previously described.³¹ Fresh esophageal squamous cancer tissue, without necrotic, infective or normal esophageal contents, was harvested from the surgically resected specimen. After washing with Hanks solution twice, tumor tissue was cut into pieces (0.5–1 mm in diameter), placed on 0.5 cm^2 gelatin sponges which were immersed in 10% FBS RPMI 1640 in each well of 24-well plates, and cultured at 37 °C with 5% CO_2 for 24 h. The A-score was recorded by the Image Analysis System according to the volumetric integral of viable samples. Then, samples were treated with 0.5 μM CCT129202 alone, 20 $\mu\text{g}/\text{mL}$ paclitaxel alone and 0.5 μM CCT129202 plus 20 $\mu\text{g}/\text{mL}$ paclitaxel. Saline and HgCl_2 (200 $\mu\text{g}/\text{mL}$) were used as negative and positive control respectively. After culturing for 92 h, 50 μL of MTT (5 mg/mL) was added and cultured for another 4 h, and the B-score was read based on the blue-stained area and the intensity of the staining. The efficacy of different treatments was evaluated according to the inhibition rate (IR). If the IR was 30% or above, it was considered to be sensitive. The inhibition rate was calculated by the following formula:

$$\text{IR} (\%) = \left[1 - \frac{\text{B-score of treated tumor/A-score of treated tumor}}{\text{B-score of control/A-score of control}} \right] \times 100\%$$

Immunohistochemical (IHC) Analysis. IHC was performed as previously described.³² Formalin-fixed esophageal tumor tissue was embedded in paraffin and cut by microtome into tissue sections (4 μm thick) for immunostaining according to standard techniques. The primary antibody was mouse anti-human ABCB1 antibody at a 1:100 dilution. A negative control for ABCB1 was performed for each specimen by omitting the primary antibody in the procedure. Subjective assessments of the intensity of membrane staining were performed according to the manufacturer's package insert.

Fluorescence Activated Cell Sorting (FACS) for Side Population (SP) Cells. The FACS was performed as previously described³³ with slight modification. In brief, A549 cells were incubated with Hoechst 33342 at a concentration of 5 $\mu\text{g}/\text{mL}$ in the presence or absence of 20 μM FTC for 90 min at 37 °C with intermittent shaking. After washing twice with

PBS, cells were resuspended and incubated with propidium iodide (PI) at a final concentration of 2 $\mu\text{g}/\text{mL}$ for gating viable cells, and then filtered using a 40 μm cell strainer to obtain a single-cell suspension. SP and NSP analysis and sorting were performed using a FACS Vantage SE (BD Biosciences, San Jose, CA).

Animals and Tumor Xenograft Experiments. Male nu/nu BALB/c mice, 5 to 6 weeks old and weighing 18 to 22 g, were bred at the animal facility of the Center of Experimental Animals, Sun Yat-Sen University (China). All animals were housed in barrier facilities and received sterilized food and water. All animal experiments were conducted with the approval of the Institutional Animal Care and Use Committee of Cancer Center of Sun Yat-Sen University.

The KBv200-inoculated nude mouse xenograft model was established as described by Fu and colleagues.²⁴ Briefly, 2×10^6 KBv200 cells were implanted subcutaneously (sc) near a shoulder of the nude mice. The mice were randomized into four groups after the tumors reached a mean diameter of 0.5 cm, and then received various regimens: (a) saline (q2d \times 4, intraperitoneally (ip)); (b) vincristine (q2d \times 4, ip, 0.2 mg/kg); (c) CCT129202 (q2d \times 4, ip, 100 mg/kg); (d) CCT129202 (q2d \times 4, ip, 100 mg/kg) followed by vincristine (q2d \times 4, ip, 0.2 mg/kg) one hour after CCT129202. The body weight, tumor volumes, feeding behavior and locomotor activity of each mouse were recorded every 2 days. When the mean tumor weight reached about 1 g, the mice were euthanized and xenografts were dissected, weighed and measured. Tumor volumes and the ratio of growth inhibition (IR) were estimated as previously described.³⁴

Ligand Structure Preparation. CCT129202 structure was built using the fragment dictionary of Maestro v9.0 and energy minimized by MacroModel program v9.7 (Schrödinger, Inc., New York, NY 2009) using the OPLSAA force field with the steepest descent followed by truncated Newton conjugate gradient protocol. The low-energy 3D structures of CCT129202 were generated with the following parameters present in LigPrep v2.3: (a) different protonation states at physiological $\text{pH} \pm 2$, (b) all possible tautomers and ring conformations. Ligand structures obtained from the LigPrep run were further used for generating 100 ligand conformations for each protonated structure using the default parameters of mixed torsional/low-mode sampling function. The conformations were filtered with a maximum relative energy difference of 5 kcal/mol to exclude redundant conformers. The output conformational search (Csearch) file containing 100 unique conformers was used as input for simulations of docking at the ATP-binding site of human ABCB1.

Protein Structure Preparation. The X-ray crystal structure of ABCB1 in the apoprotein state (PDB ID: 3G5U) and in complex with inhibitors QZ59-RRR (PDB ID: 3G6O) and QZ59-SSS (PDB ID: 3G61)³⁵ and in the ATP-bound state (PDB ID: 1MV5) obtained from the RCSB Protein Data Bank were used to build a homology model of human ABCB1. The protocol for homology modeling is essentially the same as reported before.³⁶ A refined human ABCB1 homology model was further used to generate different receptor grids by selecting QZ59-RRR (site-1) and QZ59-SSS (site-2) bound ligands, all amino acid residues known to contribute to verapamil binding (site-3), two residues (Phe728 and Val982) known to be common to sites 1–3 (site-4), and the ATP-binding site.

Table 1. Cell Survival Was Performed by MTT Assay as Described in the Experimental Section^a

compounds	IC ₅₀ ± SD (μM; fold-reversal)	
	KB	KBv200 (ABCB1)
vincristine	0.0035 ± 0.0001 (1.00)	0.746 ± 0.071 (1.00)
+ 0.125 μM CCT129202	0.0043 ± 0.0004 (0.81)	0.509 ± 0.060** (1.47)
+ 0.25 μM CCT129202	0.0040 ± 0.0053 (0.88)	0.253 ± 0.068** (2.95)
+ 0.5 μM CCT129202	0.0030 ± 0.0004 (1.17)	0.089 ± 0.005** (8.38)
+ 10 μM verapamil	0.0032 ± 0.0070 (1.09)	0.049 ± 0.003** (15.2)
doxorubicin	0.023 ± 0.001 (1.00)	4.069 ± 0.422 (1.00)
+ 0.125 μM CCT129202	0.024 ± 0.006 (0.96)	2.566 ± 0.142* (1.59)
+ 0.25 μM CCT129202	0.024 ± 0.006 (0.96)	1.689 ± 0.113** (2.41)
+ 0.5 μM CCT129202	0.018 ± 0.003 (1.28)	0.766 ± 0.041** (5.31)
+ 10 μM verapamil	0.018 ± 0.001 (1.28)	0.332 ± 0.115** (12.3)
cisplatin	2.702 ± 0.409 (1.00)	2.913 ± 0.217 (1.00)
+ 0.5 μM CCT129202	3.173 ± 0.424 (0.85)	2.942 ± 0.210 (0.99)
+ 10 μM verapamil	2.978 ± 0.388 (0.91)	2.565 ± 0.276 (1.14)
	MCF-7	MCF-7/adr (ABCB1)
doxorubicin	0.283 ± 0.006 (1.00)	7.405 ± 0.413 (1.00)
+ 0.125 μM CCT129202	0.261 ± 0.023 (1.08)	2.851 ± 0.185** (2.60)
+ 0.25 μM CCT129202	0.266 ± 0.008 (1.06)	1.884 ± 0.173** (3.93)
+ 0.5 μM CCT129202	0.247 ± 0.015 (1.15)	1.292 ± 0.046** (5.73)
+ 10 μM verapamil	0.244 ± 0.035 (1.16)	0.339 ± 0.054** (21.8)
cisplatin	32.30 ± 0.560 (1.00)	19.96 ± 0.870 (1.00)
+ 0.5 μM CCT129202	38.10 ± 6.081 (0.85)	23.45 ± 2.636 (0.85)
+ 10 μM verapamil	32.26 ± 0.321 (1.00)	16.30 ± 0.604 (1.22)
	S1	S1-M1-80 (ABCG2)
mitoxantrone	0.385 ± 0.062 (1.00)	43.28 ± 1.912 (1.00)
+ 0.125 μM CCT129202	0.387 ± 0.055 (0.99)	28.14 ± 2.363** (1.54)
+ 0.25 μM CCT129202	0.437 ± 0.054 (0.88)	8.885 ± 0.462** (4.87)
+ 0.5 μM CCT129202	0.367 ± 0.007 (1.05)	2.127 ± 0.094** (20.3)
+ 2.5 μM FTC	0.370 ± 0.038 (1.04)	0.815 ± 0.141** (53.1)
topotecan	0.481 ± 0.004 (1.00)	28.70 ± 2.628 (1.00)
+ 0.125 μM CCT129202	0.517 ± 0.066 (0.93)	21.72 ± 2.343** (1.32)
+ 0.25 μM CCT129202	0.417 ± 0.045 (1.15)	10.39 ± 1.237** (2.76)
+ 0.5 μM CCT129202	0.465 ± 0.106 (1.03)	4.234 ± 0.950** (6.78)
+ 2.5 μM FTC	0.404 ± 0.076 (1.19)	1.250 ± 0.138** (22.9)
cisplatin	17.33 ± 4.345 (1.00)	21.62 ± 4.170 (1.00)
+ 0.5 μM CCT129202	13.14 ± 0.633 (1.32)	25.74 ± 2.861 (0.84)
+ 2.5 μM FTC	18.18 ± 4.895 (0.95)	26.65 ± 0.927 (0.81)
	HL60	HL60/adr (ABCC1)
doxorubicin	0.0140 ± 0.0010 (1.00)	6.057 ± 0.493 (1.00)
+ 0.125 μM CCT129202	0.0157 ± 0.0006 (0.89)	5.701 ± 0.722 (1.06)
+ 0.25 μM CCT129202	0.0167 ± 0.0011 (0.85)	6.387 ± 0.965 (0.95)
+ 0.5 μM CCT129202	0.0163 ± 0.0006 (0.86)	5.787 ± 0.680 (1.05)
+ 50 μM MK 571	0.0133 ± 0.0012 (1.05)	0.966 ± 0.022** (6.27)

^aData are shown as the mean ± standard deviation (SD) of at least three independent experiments performed in triplicate. The fold-reversal of MDR (values given in parentheses) was calculated by dividing the IC₅₀ for cells with the chemotherapeutic drugs in the absence of inhibitor by that obtained in the presence of inhibitor. *, $p < 0.05$, **, $p < 0.01$ for values versus that obtained in the absence of CCT129202.

Docking Protocol. Conformational library of CCT129202 was docked at each of the generated grids (site-1 to site-4 as well as ATP binding site of ABCB1) using the “Extra Precision” (XP) mode of Glide program v5.5 (Schrödinger, Inc., New York, NY 2009) with the default functions. The top scoring CCT129202 conformation-ABCB1 complex was used for graphical analysis. All computations were carried out on a Dell Precision 470n dual processor with the Linux OS (Red Hat Enterprise WS 4.0).

Statistical Analysis. All experiments were carried out at least three times, and results were expressed as mean ± standard error (SE). The difference between two groups was

determined by using the two-sided Student *t* test, and comparisons among multiple groups involved one-way ANOVA. $p < 0.05$ was considered statistically significant.

RESULTS

CCT129202 Reverses ABCB1- and ABCG2-Mediated MDR in Vitro. All resistant cells were authenticated by comparing their fold resistance with that of the parental drug-sensitive cells and examining the expression level of ABC transporters (Supplementary Figure S1 in the Supporting Information). The molecular structure of CCT129202 is shown in Supplementary Figure S2A in the Supporting Information.

Table 2. Cell Survival Was Performed by MTT Assay as Described in the Experimental Section^a

compounds	IC ₅₀ ± SD (μM; fold-reversal)		
	HEK293/pcDNA3.1	HEK293/ABCG2	HEK293/ABCB1
doxorubicin	0.098 ± 0.004 (1.00)	2.668 ± 0.452 (1.00)	2.530 ± 0.020 (1.00)
+ 0.125 μM CCT129202	0.099 ± 0.019 (0.99)	0.521 ± 0.022** (5.12)	1.888 ± 0.245* (1.34)
+ 0.25 μM CCT129202	0.089 ± 0.007 (1.10)	0.156 ± 0.003** (17.1)	1.268 ± 0.363* (1.99)
+ 0.5 μM CCT129202	0.082 ± 0.009 (1.20)	0.110 ± 0.003** (24.2)	0.688 ± 0.086** (3.68)
+ 10 μM verapamil	0.101 ± 0.004 (0.97)	ND	0.148 ± 0.014** (17.1)
+ 2.5 μM FTC	0.098 ± 0.006 (1.00)	0.106 ± 0.002** (25.2)	ND
mitoxantrone	0.191 ± 0.002 (1.00)	3.622 ± 0.141 (1.00)	ND
+ 0.125 μM CCT129202	0.210 ± 0.009 (0.91)	1.484 ± 0.185** (2.44)	ND
+ 0.25 μM CCT129202	0.215 ± 0.001 (0.89)	0.624 ± 0.035** (5.80)	ND
+ 0.5 μM CCT129202	0.209 ± 0.001 (0.91)	0.326 ± 0.011** (11.1)	ND
+ 2.5 μM FTC	0.242 ± 0.028 (0.80)	0.361 ± 0.005**	ND
cisplatin	4.528 ± 0.278 (1.00)	3.601 ± 0.077 (1.00)	2.077 ± 0.267 (1.00)
+ 0.5 μM CCT129202	4.227 ± 0.169 (1.07)	3.912 ± 0.082 (0.92)	1.638 ± 0.214 (1.27)
+ 10 μM verapamil	4.553 ± 0.150 (0.99)	ND	2.415 ± 0.517 (0.86)
+ 2.5 μM FTC	4.920 ± 0.120 (0.92)	4.217 ± 0.364 (0.85)	ND

^aData are shown as the mean ± standard deviation (SD) of at least three independent experiments performed in triplicate. The fold-reversal of MDR (values given in parentheses) was calculated by dividing the IC₅₀ for cells with the chemotherapeutic drugs in the absence of inhibitor by that obtained in the presence of inhibitor. *, $p < 0.05$, **, $p < 0.01$ for values versus that obtained in the absence of CCT129202. ND, no data.

Prior to examining the effect of CCT129202 on reversing MDR in cancer cells, the cytotoxicity of CCT129202 was determined by MTT assay. The IC₅₀ values were 1.724 ± 0.250 , 7.023 ± 0.306 , 0.987 ± 0.054 , 6.130 ± 0.209 , 3.647 ± 0.192 , 25.66 ± 2.487 , 1.464 ± 0.134 and 6.528 ± 1.355 μM for KB, KBv200, S1, S1-M1-80, MCF-7, MCF-7/adr, HL60 and HL60/adr, respectively (Supplementary Figure S2 in the Supporting Information). In transfected cell lines, the IC₅₀ values were >4 μM for HEK293/pcDNA3.1, HEK293/ABCB1 and HEK293/ABCG2-T7 (Supplementary Figure S2 in the Supporting Information). CCT129202, at a concentration up to 0.5 μM, was of no obvious cytotoxicity with more than 90% of cells viable in all cell lines tested. The IC₅₀ values of chemotherapeutic drugs in combination with various concentrations of CCT129202 in drug-sensitive, resistant cells, and in transfected cells are shown in Tables 1 and 2. CCT129202 exhibited a concentration dependent increase of the cytotoxicity of ABCB1 or ABCG2 substrate drugs in ABCB1-overexpressing cells (KBv200 and MCF-7/adr) and ABCG2-overexpressing cells (S1-M1-80). Furthermore, CCT129202 also significantly reversed ABCB1-mediated resistance to doxorubicin in ABCB1 transfected HEK293/ABCB1 cells. Importantly, 0.5 μM CCT129202 almost completely reversed the ABCG2-mediated resistance to doxorubicin and mitoxantrone in HEK293/ABCG2-T7 cells (Table 2). In contrast, CCT129202 did not alter the cytotoxicity of chemotherapeutic agents in their parental sensitive cell lines and ABCC1-overexpressing HL60/adr cells (Table 1). Furthermore, considering that cisplatin is not a substrate of ABCB1 or ABCG2, we used cisplatin as a negative control drug to examine the substrate specificity of transporters and found that CCT129202 did not alter the IC₅₀ values of cisplatin in all cell lines (Table 1 and 2).

On the other hand, we performed a study about the silencing of ABCB1 in KBv200 cells. ABCB1-siRNA-2 and ABCB1-siRNA-3 effectively downregulated the expression of ABCB1 in KBv200 cells (Supplementary Figure S3 in the Supporting Information). Compared with the control, ABCB1-siRNA-2 and ABCB1-siRNA-3 decreased the IC₅₀ of doxorubicin from 4.625 μM to 1.345 μM and 1.191 μM (Supplementary Table

S1 in the Supporting Information), respectively, which is consistent with our previous report.²⁵ Moreover, CCT129202 only slightly enhanced the cytotoxicity of doxorubicin in ABCB1 silent KBv200 cells. The IC₅₀ value of doxorubicin was decreased from 1.345 to 0.740 μM in KBv200/ABCB1-siRNA-2 cells and from 1.191 to 0.765 μM in KBv200/ABCB1-siRNA-3 cells (Supplementary Figure S3 and Table S1 in the Supporting Information).

Our in vitro study reveals that CCT129202 can specifically reverse ABCB1 and ABCG2-mediated MDR in drug-resistant cancer cells and gene transfected cells.

CCT129202 Reverses ABCB1-Mediated MDR in Vivo.

The ABCB1-overexpressing KBv200 cell xenograft model in nude mice was established to examine the efficacy of CCT129202 on reversal of the resistance to vincristine in vivo. The weight of tumors removed from sacrificed mice was 1.387 ± 0.731 , 1.169 ± 0.639 , 1.033 ± 0.714 and 0.665 ± 0.367 g for saline, vincristine alone, CCT129202 alone, and combination groups, respectively. There was no significant difference in tumor size and weight among animals treated with saline, CCT129202, and vincristine, indicating that the KBv200 cells are resistant to vincristine in vivo. However, the combination of CCT129202 and vincristine group produced a significant inhibition of tumor growth compared with animals treated with saline, vincristine or CCT129202 alone ($p < 0.05$, Figures 1A and 1B). The inhibition rate in the combination group was 50.7%. Furthermore, at the dosage level tested, no mortality or apparent decrease in body weight was observed in the combination treatment group (Figure 1C), indicating that the combination regimen was tolerated by the mice.

CCT129202 Reverses MDR in ex Vivo. Considering that CCT129202 effectively reversed ABCB1-mediated MDR both in vitro and in vivo, we further determined the potential effect of CCT129202 on the reversal of MDR in cultured esophageal squamous tumor tissue with ABCB1 overexpression. IHC and TECIA were performed in 20 esophageal cancer samples (clinical characteristics of the patients shown in Supplementary Table S2 in the Supporting Information). IHC analysis showed the positive expression of ABCB1 in 3 samples (15%), and negative in 17 (85%). The positive samples showed cytoplasmic

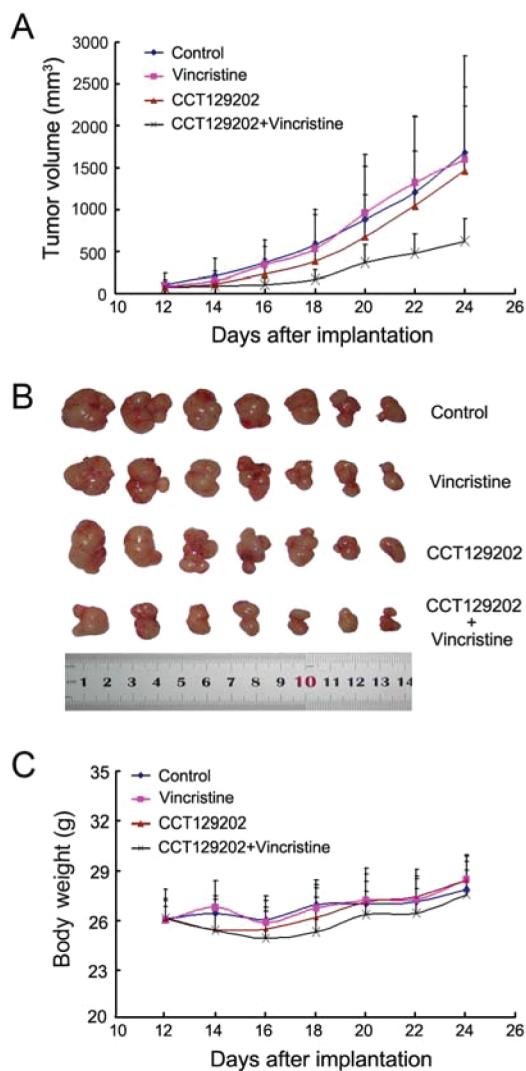


Figure 1. Potentiation of the antitumor effects of vincristine by CCT129202 in a KBv200 xenograft model in nude mice. The changes of tumor volumes (A and B) and body weight (C) in groups with different treatments are shown. Tumors were randomized according to tumor size and body weight, and treatments were initiated on day 12 as follows: control (vehicle alone); vincristine (q2d \times 4, ip, 0.2 mg/kg); CCT129202 (q2d \times 4, ip, 100 mg/kg); vincristine (q2d \times 4, ip, 0.2 mg/kg) plus CCT129202 (q2d \times 4, ip, 100 mg/kg, given an hour before vincristine administration). Points, mean tumor volume or body weight for each group of 7 mice after implantation; bars, SD. (B) Photo of tumors dissected on day 24 postinoculation.

and membranous expression of ABCB1. The representative examples of immunostaining of ABCB1 ranging from negative (–) to very strongly positive (+++) were shown in Figure 2A. The efficacy of paclitaxel was performed by TECIA as described in the Experimental Section. All samples treated with 0.5 μ M CCT129202 alone revealed no apparent growth inhibition (IR < 10%). Importantly, CCT129202 significantly enhanced the efficacy of paclitaxel on the tumor inhibition in ABCB1-positive group, and the IR of paclitaxel with and without 0.5 μ M CCT129202 was 64.91 ± 7.499 and 19.21 ± 8.221 (%), respectively ($p = 0.01$). However, no significant difference was observed in the ABCB1-negative group (Figure 2C). These results suggested that CCT129202 enhanced the efficacy of paclitaxel in ABCB1-mediated drug resistance in ex vivo.

CCT129202 Potentiates the Anticancer Activity of Doxorubicin in Side Population (SP) Cells.

Since the expressions of ABC transporters such as ABCG2 are the putative markers of SP cells and may contribute to drug resistance in cancer stem cells, the effect of CCT129202 on the enhancement of chemotherapeutic agent in SP and non-side population (NSP) cells was investigated. ABCG2 expression was found in SP cells but not in NSP cells (Supplementary Figure S4A in the Supporting Information). SP cells of A549 were isolated (Figure 2D) and then treated with full-range concentrations of CCT129202 (Figure 2E). Based on these concentration–response curves, we chose 0.25 μ M CCT129202 as the concentration of combination with doxorubicin. Compared with NSP cells, the IC_{50} value of doxorubicin was 2.39-fold higher in SP cells. CCT129202 significantly abolished the drug-resistant ability of SP cells to doxorubicin but did not alter IC_{50} value of doxorubicin in NSP cells (Figure 2F).

CCT129202 Increases the Accumulation of Doxorubicin and Rhodamine 123 in Cells Overexpressing ABCB1 and ABCG2.

After recognizing the efficacy of CCT129202 in reversing MDR, we further investigated the impact of this drug on ABCB1 and ABCG2 functions. The effect of CCT129202 on the drug-efflux function of ABCB1 and ABCG2 was evaluated by assays of accumulation of their respective substrates, doxorubicin and rhodamine 123. CCT129202 significantly increased the accumulation of doxorubicin and rhodamine 123 in ABCB1-overexpressing KBv200 and MCF-7/adr cells as well as ABCG2-overexpressing S1-M1-80 cells in a dose-dependent manner (Supplementary Figure S5 in the Supporting Information, Figure 3A,B). In the presence of 0.125, 0.25, 0.5 μ M CCT129202, the intracellular accumulation of doxorubicin was increased 1.39-, 1.67- and 2.36-fold in KBv200, respectively; 1.37-, 1.59- and 2.27-fold in MCF-7/adr, respectively; 1.46-, 3.08- and 4.16-fold higher in S1-M1-80 cells, respectively (Figure 3A). Similarly, in the presence of 0.125, 0.25, 0.5 μ M CCT129202, the intracellular accumulation of rhodamine 123 was increased 1.33-, 1.51- and 1.79-fold in KBv200, respectively; 1.45-, 2.02- and 2.48-fold higher in MCF-7/adr, respectively; 1.53-, 1.83- and 3.88-fold higher in S1-M1-80 cells, respectively (Figure 3B). In contrast, CCT129202 did not alter the levels of doxorubicin and rhodamine 123 in their parental KB, MCF-7 and S1 cells. In summary, the results suggest that CCT129202 inhibits ABCB1- and ABCG2-mediated drug efflux in MDR cells.

CCT129202 Inhibits the ATPase Activity of ABCB1.

The drug-efflux function of ABC transporter is linked to ATP hydrolysis, and thus ATPase activity can be reflected by ATP consumption.³⁷ To determine the effect of CCT129202 on the ATPase activity of ABCB1, we measured ABCB1-mediated ATP hydrolysis using various concentrations of CCT129202. The result revealed that CCT129202 decreased verapamil-stimulated ATPase activity of ABCB1 in a dose-dependent manner (Figure 3C). Consequently, CCT129202 is an inhibitor of the ATPase activity of ABCB1.

CCT129202 Does Not Significantly Alter the Expression of ABCB1 and ABCG2 at Protein or mRNA Levels.

Considering that the change of the function of ABC transporters may result from a downregulation of ABC expression, we further investigated the effect of CCT129202 on the expression of ABCB1 and ABCG2 at protein and mRNA levels. Western blotting was performed to determine the expression of proteins, and mRNA levels were tested by

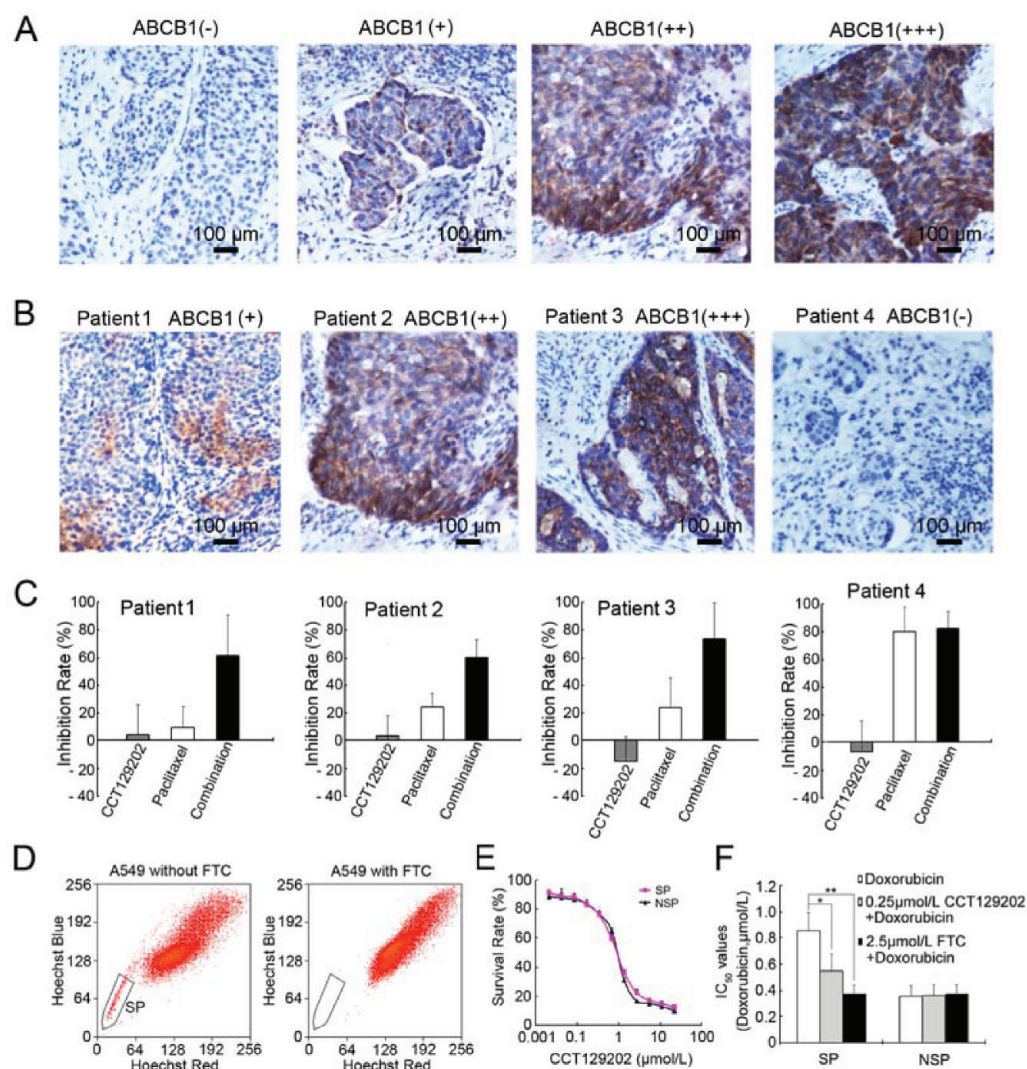


Figure 2. CCT129202 enhanced the anticancer activity of paclitaxel in human esophageal squamous cancer tissue expressing ABCB1 and that of doxorubicin in side population cells of A549. The expressions of ABCB1 (A) tested by IHC ($\times 400$) in human esophageal cancer tissue were demonstrated. Samples from three patients showed positive ABCB1 expression (B) and an enhancement of efficacy of paclitaxel by CCT129202 (C). The regimen was described as follows: CCT129202 alone; paclitaxel alone; and combined treatment (paclitaxel plus CCT129202, given an hour before paclitaxel administration). Staining intensities were graded as follows: (–) negativity; (+) low-intensity; (++) moderate-intensity; (+++) high-intensity. The A549 cells were stained with Hoechst 33342 in the presence (D, right) or absence (D, left) of $20 \mu\text{M}$ FTC and analyzed by flow cytometry. Gated on forward and side scatter to exclude debris, Hoechst red versus Hoechst blue was used to sort SP cells. (E) The cytotoxicity of CCT129202 alone was performed by MTT assay in SP and NSP cells of A549. (F) Induction of 50% cell death in SP and NSP cells by doxorubicin with or without $0.25 \mu\text{M}$ CCT129202 or $2.5 \mu\text{M}$ FTC. Columns, means of triplicate determinations; *, $p < 0.05$; **, $p < 0.01$, compared with doxorubicin treatment.

reverse transcription (RT) and quantitative real-time PCR. The results revealed that CCT129202, at concentrations of 0.125, 0.25, $0.5 \mu\text{M}$, did not significantly alter the expression of ABCB1 at KBv200 cells and ABCG2 at S1-M1-80 cells (Figure 4A–C), which indicated that CCT129202 reversed MDR by inhibiting the function of ABCB1 and ABCG2 rather than downregulating levels of their expressions.

Effect of CCT129202 on the Aurora Kinases.

CCT129202 is a novel inhibitor of Aurora kinases and can effectively induce G2/M arrest (an Aurora A effect) and polyploidy (an Aurora B effect).⁹ Therefore, we measured the effect of CCT129202 on the activity of Aurora kinases. The distribution in cell cycle phases was measured at 0, 0.5, and $2 \mu\text{M}$ CCT129202 by flow cytometry in KBv200 cells and its parental KB cells. As shown in Figures 4D and 4E, $0.5 \mu\text{M}$

CCT129202 did not significantly alter the cell cycle of KBv200 and KB cells, and the arrest of cells in G2/M was not increased until a concentration up to $2 \mu\text{M}$. Also, $0.5 \mu\text{M}$ CCT129202 did not significantly increase the percentage of cells with polyploidy (Supplementary Figures S6A and S6B in the Supporting Information). Subsequently, we tested the expressions of Aurora kinase related proteins. We found that CCT129202 did not change the expressions of Aurora A, p-Aurora A, p-histone H3, p21 and c-Myc at concentrations until $2 \mu\text{M}$ in KBv200 cells (Figure 4F and Supplementary Figure S6C in the Supporting Information). The above results revealed that CCT129202 had no significant effect on cell cycle and the kinase activity of Aurora kinase A and B at concentrations used in resistance reversal experiments in vitro.

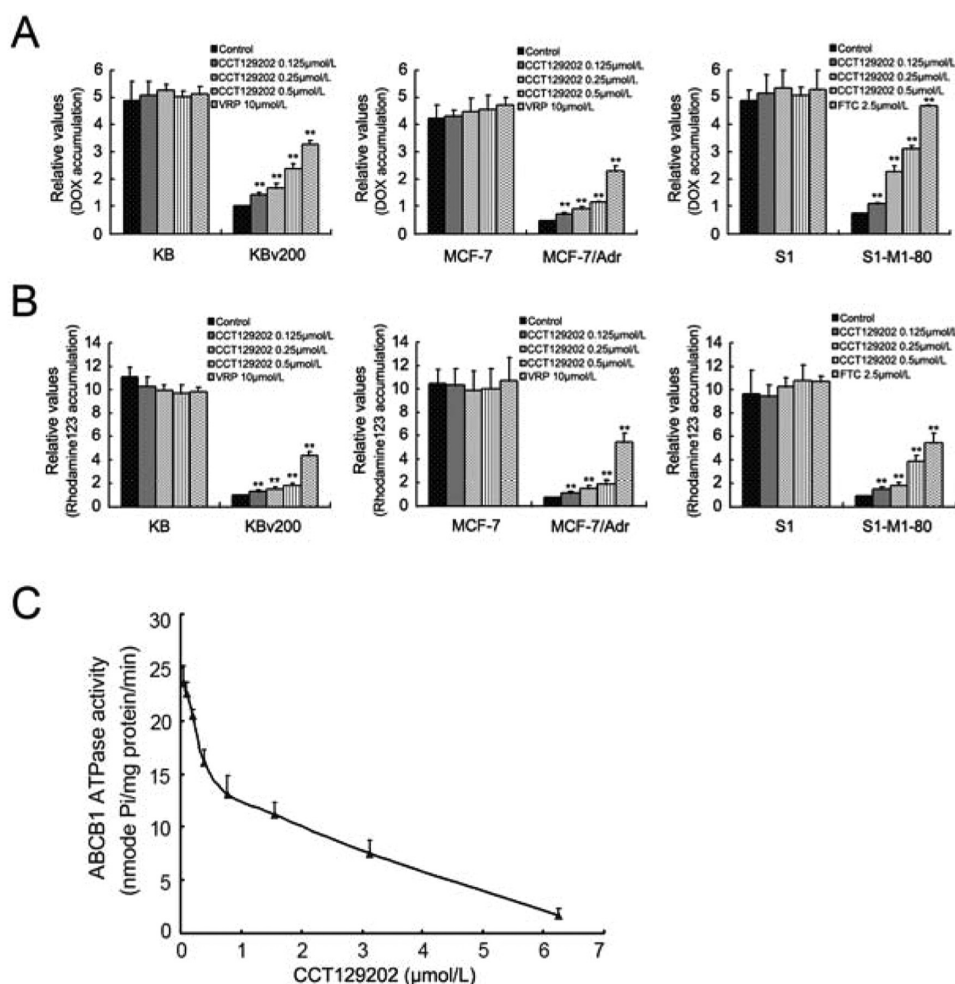


Figure 3. Effect of CCT129202 on the accumulation of doxorubicin and Rhodamine 123 and on the ATPase activity of ABCB1. Accumulation of doxorubicin (A) and Rhodamine 123 (B) was measured by flow cytometric analysis after the cells were incubated with or without CCT129202, verapamil (VRP), or fumitremorgin C (FTC). All were performed as described in the Experimental Section. Columns, means of triplicate determinations; bars, SD. **, $p < 0.01$, versus the control. Independent experiments were performed at least three times, and a representative result is shown. ABCB1 ATPase assay was performed according to the instruction of Pgp-Glo Assay Systems. CCT129202 inhibited verapamil-stimulated ATPase activity of ABCB1 in a dose-dependent manner (C). Independent experiments were performed at least three times, and a representative result is shown.

We also detected the effect of CCT129202 on activities of Aurora A and B in vivo by examining an increased expression of MPM2/FoxM1 (an Aurora A effect) or the increase in multinucleated giant cells (an Aurora B effect). There was no significant difference of the expression of MPM2/FoxM1 and the percentage of multinucleated giant cells between the control group and CCT129202 alone group (Supplementary Figure S7 in the Supporting Information). These results suggest that CCT129202 does not inhibit the activity of Aurora A and Aurora B under the concentration of reversal MDR.

Binding Model of CCT129202 to ABCB1. To understand the molecular interactions of CCT129202 with ABCB1 using the homology model of human ABCB1,³⁶ we performed glide docking using ABCB1-QZ59-RRR (site-1), ABCB1-QZ59-SSS (site-2), ABCB1-verapamil (site-3), and a site common to the above three sites (site-4)³⁵ and the ATP-binding site. The binding energy data (Glide scores in kcal/mol for CCT129202 at site-1 to site-4 and ATP binding site are -7.83 , -6.47 , -7.43 , -7.75 and -2.88 , respectively) suggest that site-1 is the most favorable one. Hence, further simulations and discussion are

mainly focused on the binding interactions of CCT129202 at site-1.

The predicted binding conformation of CCT129202 within the large hydrophobic drug binding cavity (site-1) of human ABCB1 is shown in Figure 5. The *p*-dimethylaminophenyl substituent of CCT129202 is extensively stabilized through hydrophobic side chains of Leu65, Met68, Met69, Phe72, Phe336, Ile340, Phe957 and Phe978. Whereas the imidazopyridine ring forms hydrophobic interactions with the side chains of Phe732, Phe336, Leu975, Phe978 and Val982, the piperazine ring interacts through hydrophobic contacts with the side chains of Phe336, Phe728 and Val982. The carbonyl oxygen atom of the acetamide group is located such that it may form hydrogen bonding interaction with the side chains of both Tyr307 and Gln725 ($-\text{CO}\cdots\text{HO-Tyr307}$, 2.1 Å) and Gln725 ($-\text{CO}\cdots\text{H}_2\text{NOC-Gln725}$, 2.1 Å), thus resulting in conformational locking of these two residues. The thiazole ring seems to be stabilized by hydrophobic interactions with residues Leu304 and Tyr307. It is interesting to note that CCT129202 assumed an inverted V-shape conformation within the site-1 of human

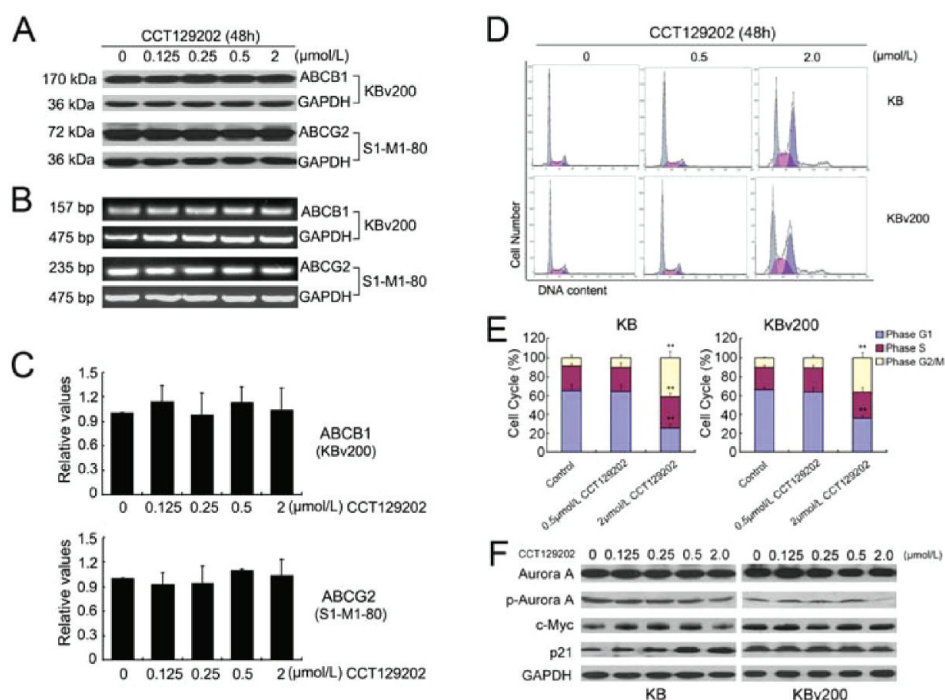


Figure 4. Effect of CCT129202 on ABCB1 and ABCG2 expression and the function of Aurora kinase. CCT129202 did not alter the expressions of ABCB1 and ABCG2 at protein level (A) and mRNA level (B, C). The change at mRNA level was determined by RT-PCR (B) and quantitative real-time PCR (C). CCT129202, at concentrations up to 0.5 μM , did not alter the cell cycle distribution of KB and KBv200 cells for 24 h (D, E). The expression of cell cycle regulated proteins after CCT129202 treatment was assessed by Western blot (F), and a representative result from at least three independent experiments is shown. Histogram analyses are shown as means \pm SD. **, $p < 0.01$ vs the control.

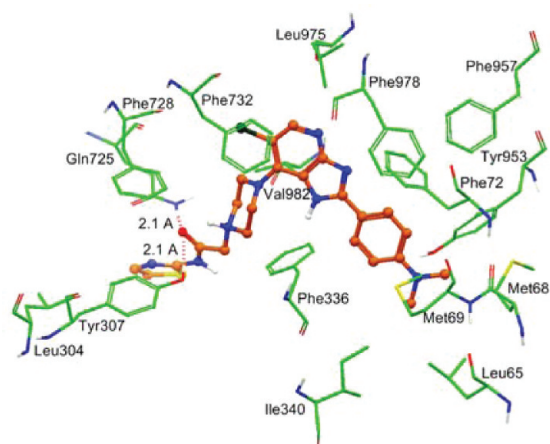


Figure 5. XP-Glide predicted binding conformation of CCT129202 within the site-1 of human ABCB1. Important amino acids of ABCB1 contacting CCT129202 are depicted as tubes with the atoms colored as follows: carbon, green; hydrogen, white; nitrogen, blue; oxygen, red; sulfur, yellow; whereas the inhibitor is shown as a ball and stick model with the same color scheme as above except carbon atoms are indicated by orange color and the chloro group by dark green.

ABCB1, a shape reminiscent of the conformation of Aurora A kinase inhibitors when docked with Aurora A.

DISCUSSION

MDR is a phenomenon of acquired resistance of cancer cells to chemotherapeutics with different chemical structures and different modes of action. Complex mechanisms contribute to the development of MDR. The overexpression of a series of trans-membrane proteins with the ability of extruding diverse

drugs out of cancer cells, such as the ATP-binding cassette (ABC) transporters, is considered as a key factor for MDR.¹ Small molecule inhibitors targeting MDR cancer cells may be an effective therapy to reverse the resistance to chemotherapy.

Many small molecule tyrosine kinase inhibitors target the ATP-binding pockets of various kinases. CCT129202 is a small-molecule inhibitor with potent and selective activity against pan-Aurora kinase compared with other kinases, and shows anticancer activity in various cancer cells and in HCT116 tumor xenografts in athymic mice.⁹ In this study, we explored the effects of CCT129202 on the reversal of MDR and its interaction with ABC transporters.

Our study first found that CCT129202 had potent resistance reversal effect of ABCB1 and ABCG2 overexpressing MDR cells (Tables 1 and 2). CCT129202 significantly enhanced the cytotoxicity of conventional antineoplastic drugs and increased the accumulation of doxorubicin and rhodamine 123 in MDR cell lines overexpressing ABCB1 and ABCG2 (Tables 1 and 2, Figure 3A,B), but not in their drug-sensitive parental cells with undetectable ABC transporters expression. However, CCT129202 had no apparent effect on ABCC1 overexpressing HL60/adr cells, its drug-sensitive HL60 cells and the cytotoxicity of cisplatin, a nonsubstrate of both ABCB1 and ABCG2 (Table 1). Furthermore, the effect of CCT129202 on reversing MDR was decreased when the expression of ABCB1 was downregulated by ABCB1-siRNA in KBv200 cells (Supplementary Figure S3 and Table S1 in the Supporting Information). These results suggest that the reversal of MDR by CCT129202 was probably associated with inhibiting their efflux function.

The favorable *in vitro* results prompted us to examine whether the effect of CCT129202 *in vitro* can be extended to an *in vivo* paradigm. The combination of CCT129202 and

vincristine apparently enhanced antitumor activity of vincristine in an ABCB1-overexpressing xenograft model in nude mice (Figure 1A and B). And no significant difference of adverse effects was observed as monitored by the body weight and physical activity of the mice among four groups (Figure 1C).

Paclitaxel-based agents were used to treat a range of solid tumors, and considered as the first-line chemotherapy for metastatic or locally advanced esophageal carcinoma according to NCCN guidelines (2011).³⁸ However, the anticancer activity is often limited by the appearance of MDR. We hypothesized that the CCT129202 in combination with paclitaxel may reverse the resistance to paclitaxel. TECIA results revealed that esophageal squamous tumor samples with positive ABCB1 expression exhibited paclitaxel resistance compared to that with negative expression of ABCB1 (Figure 2), and CCT129202 in combination with paclitaxel significantly reversed the resistance in ABCB1-positive tissues (Figure 2). These *ex vivo* results hinted that CCT129202 may be a promising agent to reverse clinical drug resistance associated with ABCB1.

According to the cancer stem cell hypothesis, clinical resistance to chemotherapy may result from the presence of a small, surviving population of cancer stem-like cells.³⁹ The expression of ABCG2 is a feature of stem-like cells, and has been exploited to isolate the side population (SP) and non-side population (NSP) cells.⁴⁰ We found that ABCG2 was expressed in SP cells, but not in NSP cells (Supplementary Figure S4A in the Supporting Information). A 2.39-fold resistance to doxorubicin was also found in SP cells compared with NSP cells, and the resistance was abrogated by CCT129202 (Figure 2F). These data suggest that CCT129202 could also target to SP cells and enhance the cytotoxicity of doxorubicin.

Binding of ATP to the nucleotide-binding sites of ABC transporters and releasing energy from the hydrolysis of ATP by ATPase are critical for the transporters to effectively transport their substrates,⁴¹ and thus the change of ATPase activity of the transporters directly reflects their transport activity. Some tyrosine kinase inhibitors (TKIs) such as lapatinib,⁷ erlotinib⁴² and apatinib,³⁴ function as MDR modulators, and can stimulate the ATPase activity of ABC transporters while some others, such as BIBF 1120, can inhibit the ATPase activity and the function of ABCB1 transporter.²⁸ We found that CCT129202 inhibited the ATPase activity in the ABCB1-expressing membrane (Figure 3C) while it had no effects on the expression of ABCB1 and ABCG2 at mRNA and protein levels (Figure 4A–C). The results suggested that CCT129202 can reverse ABCB1-mediated MDR by inhibiting ATP hydrolysis by ABCB1.

Chan and colleagues reported that CCT129202, at a certain concentration, can induce G2/M arrest and polyploidy in cancer cells.⁹ To elucidate whether the reversal effect in ABCB1- and ABCG2-mediated MDR cells was related to the altered activation of Aurora kinases, cell cycle and activation of Aurora kinases were determined. No significant changes in cell cycle were observed in KB and KBv200 cells until 2.0 μ M CCT129202 (Figures 4D and 4E). Besides, CCT129202 at its reversal concentrations did not alter the expression of total Aurora A and p-Aurora A, as well as its downstream target proteins p21 and c-Myc in KBv200 cells (Figure 4F). Moreover, CCT129202 did not significantly induce polyploidy or inhibit the phosphorylation of histone H3, all of which are hallmarks of Aurora B inhibition (Supplementary Figure S6 in the Supporting Information). We detected the effect of

CCT129202 on activities of Aurora A or B in the *in vivo* studies by an increase expression of MPM2/FoxM1 (an aurora A effect) or the increase in multinucleated giant cells (aurora B effect). Consistent with the *in vitro* results, CCT129202 did not inhibit the activities of Aurora A and Aurora B (Supplementary Figure S7 in the Supporting Information). These findings suggest that inhibition of Aurora kinase pathway is not involved in the reversal of ABCB1- and ABCG2-mediated MDR by CCT129202.

The structure of CCT129202 represents two pharmacophoric features such as aromatic/heteroaromatic ring centers and positively charged ionizable tertiary amine of the piperazine ring that are essential and reported for ABCB1 inhibitors.⁴³ Moreover, various QSAR analyses^{44–46} on P-gp inhibitors have clearly demonstrated the contribution of lipophilicity toward P-gp inhibitory activity. The best docking site-1 on human ABCB1 was located in the hydrophobic transmembrane domains, and CCT129202 exhibited a calculated QikProp v3.2 log *P* value of 3.47. Thus it is not surprising that CCT129202 favorably binds in the large hydrophobic vacuum cleaner drug-binding cavity of human ABCB1.

Based on the reported structure–activity relationship studies on imidazopyridine class of Aurora A kinase inhibitors,^{47,48} it seems that both the *p*-dimethylamino substituent on the phenyl ring and the thiazole ring, being solvent exposed in the Aurora A kinase active site, tolerate various substituents and may be considered as potential sites for further structure optimization to maintain Aurora A kinase inhibitory activity with simultaneous improvement in ABCB1 inhibitory activity. The present study suggests that CCT129202 may be useful as a parent compound to search for analogues that can inhibit both Aurora A kinase and ABC transporters, and this CCT129202 docking model and site-1 topological environment will form the theoretical basis for future optimization of CCT129202.

Further docking analysis of Aurora A kinase inhibitors (AMG900, PF03814735, CCT137690, R763, AT9283, SNS314, GSK1070916, MLN8054, and MLN8237) that are currently in various stages of clinical trials indicated that some of these (e.g., AMG900, PF03814735, CCT137690, R763, and AT9283) could be potential inhibitors of ABCB1 (data not shown). These inhibitors will be explored for their MDR reversal potential in our future study.

In summary, our results show that CCT129202 can effectively reverse ABCB1- and ABCG2-mediated MDR via inhibiting the efflux function of these transporters, resulting in an increase in intracellular concentration of conventional chemotherapeutic agents. The significant MDR reversal effect by CCT129202 provides the preclinical rationale for upcoming clinical trials about the combination of CCT129202 with other antineoplastic drugs to overcome clinical drug resistance and target cancer stem cells and enhance the efficacy of chemotherapeutic agents.

■ ASSOCIATED CONTENT

📄 Supporting Information

Additional figures and tables as discussed in the text. This material is available free of charge via the Internet at <http://pubs.acs.org>.

■ AUTHOR INFORMATION

Corresponding Author

*L.-w.F.: State Key Laboratory of Oncology in South China, Cancer Center, Sun Yat-Sen University, Guangzhou, 510060,

China; phone, +86-(20)-873-431-63; fax, +86-(20)-873-431-70; e-mail, fulw@mail.sysu.edu.cn. C.C.: The First Affiliated Hospital of Sun Yat-Sen University, 58 Zhongshan 2nd Road, Guangzhou, 510080, China; phone, +86-(20)-87755766-8782; fax, +86-(20)-873-327-50; e-mail, drchengchao@yahoo.com.cn.

Author Contributions

‡C.C. and Z.-g.L. contributed equally to this work.

Notes

The authors declare no competing financial interest.

ACKNOWLEDGMENTS

We thank Drs. S. E. Bates and R. W. Robey (National Cancer Institute, NIH, Bethesda, MD) for the ABCG2 expressing cell line S1-M1-80 and ABCB1 and ABCG2 transfected cell lines, and Sai-Ching J. Yeung (The University of Texas M. D. Anderson Cancer Center, Houston, Texas) for critical reading of the manuscript. The work was supported by grants from China 863 Project Foundation (No. 2006AA02A404 to L.-w.F.), China 973 Project Foundation (No. 2010CB833603 to L.-w.F.), China National Natural Sciences Foundation (No. 30801136 and No. 81171125 to C.C.), and the Foundation from State Key Laboratory of Oncology in Southern China.

REFERENCES

- (1) Sparreboom, A.; Danesi, R.; Ando, Y.; Chan, J.; Figg, W. D. Pharmacogenomics of ABC transporters and its role in cancer chemotherapy. *Drug Resist. Updates* **2003**, *6* (2), 71–84.
- (2) Glavinas, H.; Krajcsi, P.; Cserepes, J.; Sarkadi, B. The role of ABC transporters in drug resistance, metabolism and toxicity. *Curr. Drug Delivery* **2004**, *1* (1), 27–42.
- (3) Dean, M.; Rzhetsky, A.; Allikmets, R. The human ATP-binding cassette (ABC) transporter superfamily. *Genome Res.* **2001**, *11* (7), 1156–66.
- (4) Sarkadi, B.; Homolya, L.; Szakacs, G.; Varadi, A. Human multidrug resistance ABCB and ABCG transporters: participation in a chemoinnate defense system. *Physiol. Rev.* **2006**, *86* (4), 1179–236.
- (5) Al-Ejeh, F.; Smart, C. E.; Morrison, B. J.; Chenevix-Trench, G.; Lopez, J. A.; Lakhani, S. R.; Brown, M. P.; Khanna, K. K. Breast cancer stem cells: treatment resistance and therapeutic opportunities. *Carcinogenesis* **2011**, *32* (5), 650–8.
- (6) Subramaniam, D.; Ramalingam, S.; Houchen, C. W.; Anant, S. Cancer stem cells: a novel paradigm for cancer prevention and treatment. *Mini-Rev. Med. Chem.* **2010**, *10* (5), 359–71.
- (7) Dai, C. L.; Tiwari, A. K.; Wu, C. P.; Su, X. D.; Wang, S. R.; Liu, D. G.; Ashby, C. R., Jr.; Huang, Y.; Robey, R. W.; Liang, Y. J.; Chen, L. M.; Shi, C. J.; Ambudkar, S. V.; Chen, Z. S.; Fu, L. W. Lapatinib (Tykerb, GWS72016) reverses multidrug resistance in cancer cells by inhibiting the activity of ATP-binding cassette subfamily B member 1 and G member 2. *Cancer Res.* **2008**, *68* (19), 7905–14.
- (8) Jagiello-Gruszfeld, A.; Tjulandin, S.; Dobrovolskaya, N.; Manikhas, A.; Pienkowski, T.; DeSilvio, M.; Ridderheim, M.; Abbey, R. A single-arm phase II trial of first-line paclitaxel in combination with lapatinib in HER2-overexpressing metastatic breast cancer. *Oncology* **2010**, *79* (1–2), 129–35.
- (9) Chan, F.; Sun, C.; Perumal, M.; Nguyen, Q. D.; Bavetsias, V.; McDonald, E.; Martins, V.; Wilsher, N. E.; Raynaud, F. L.; Valenti, M.; Eccles, S.; Te Poele, R.; Workman, P.; Aboagye, E. O.; Linardopoulos, S. Mechanism of action of the Aurora kinase inhibitor CCT129202 and in vivo quantification of biological activity. *Mol. Cancer Ther.* **2007**, *6* (12 Part 1), 3147–57.
- (10) Zhou, H.; Kuang, J.; Zhong, L.; Kuo, W. L.; Gray, J. W.; Sahin, A.; Brinkley, B. R.; Sen, S. Tumour amplified kinase STK15/BTAK induces centrosome amplification, aneuploidy and transformation. *Nat. Genet.* **1998**, *20* (2), 189–93.

(11) Jeng, Y. M.; Peng, S. Y.; Lin, C. Y.; Hsu, H. C. Overexpression and amplification of Aurora-A in hepatocellular carcinoma. *Clin. Cancer Res.* **2004**, *10* (6), 2065–71.

(12) Landen, C. N., Jr.; Lin, Y. G.; Immaneni, A.; Deavers, M. T.; Merritt, W. M.; Spannuth, W. A.; Bodurka, D. C.; Gershenson, D. M.; Brinkley, W. R.; Sood, A. K. Overexpression of the centrosomal protein Aurora-A kinase is associated with poor prognosis in epithelial ovarian cancer patients. *Clin. Cancer Res.* **2007**, *13* (14), 4098–104.

(13) Gully, C. P.; Zhang, F.; Chen, J.; Yeung, J. A.; Velazquez-Torres, G.; Wang, E.; Yeung, S. C.; Lee, M. H. Antineoplastic effects of an Aurora B kinase inhibitor in breast cancer. *Mol. Cancer* **2010**, *9*, 42.

(14) Ditchfield, C.; Johnson, V. L.; Tighe, A.; Ellston, R.; Haworth, C.; Johnson, T.; Mortlock, A.; Keen, N.; Taylor, S. S. Aurora B couples chromosome alignment with anaphase by targeting BubR1, Mad2, and Cenp-E to kinetochores. *J. Cell Biol.* **2003**, *161* (2), 267–80.

(15) Soncini, C.; Carpinelli, P.; Gianellini, L.; Fancelli, D.; Vianello, P.; Rusconi, L.; Storici, P.; Zugnoni, P.; Pesenti, E.; Croci, V.; Ceruti, R.; Giorgini, M. L.; Cappella, P.; Ballinari, D.; Sola, F.; Varasi, M.; Bravo, R.; Moll, J. PHA-680632, a novel Aurora kinase inhibitor with potent antitumoral activity. *Clin. Cancer Res.* **2006**, *12* (13), 4080–9.

(16) Harrington, E. A.; Bebbington, D.; Moore, J.; Rasmussen, R. K.; Ajose-Adeogun, A. O.; Nakayama, T.; Graham, J. A.; Demur, C.; Hercend, T.; Diu-Hercend, A.; Su, M.; Golec, J. M.; Miller, K. M. VX-680, a potent and selective small-molecule inhibitor of the Aurora kinases, suppresses tumor growth in vivo. *Nat. Med.* **2004**, *10* (3), 262–7.

(17) Lin, Y. G.; Immaneni, A.; Merritt, W. M.; Mangala, L. S.; Kim, S. W.; Shahzad, M. M.; Tsang, Y. T.; Armaiz-Pena, G. N.; Lu, C.; Kamat, A. A.; Han, L. Y.; Spannuth, W. A.; Nick, A. M.; Landen, C. N., Jr.; Wong, K. K.; Gray, M. J.; Coleman, R. L.; Bodurka, D. C.; Brinkley, W. R.; Sood, A. K. Targeting aurora kinase with MK-0457 inhibits ovarian cancer growth. *Clin. Cancer Res.* **2008**, *14* (17), 5437–46.

(18) Wang, R. B.; Kuo, C. L.; Lien, L. L.; Lien, E. J. Structure-activity relationship: analyses of p-glycoprotein substrates and inhibitors. *J. Clin. Pharm. Ther.* **2003**, *28* (3), 203–28.

(19) Chen, L. M.; Wu, X. P.; Ruan, J. W.; Liang, Y. J.; Ding, Y.; Shi, Z.; Wang, X. W.; Gu, L. Q.; Fu, L. W. Screening novel, potent multidrug-resistant modulators from imidazole derivatives. *Oncol. Res.* **2004**, *14* (7–8), 355–62.

(20) Mi, Y.; Lou, L. ZD6474 reverses multidrug resistance by directly inhibiting the function of P-glycoprotein. *Br. J. Cancer* **2007**, *97* (7), 934–40.

(21) Fu, L.; Liang, Y.; Deng, L.; Ding, Y.; Chen, L.; Ye, Y.; Yang, X.; Pan, Q. Characterization of tetrandrine, a potent inhibitor of P-glycoprotein-mediated multidrug resistance. *Cancer Chemother. Pharmacol.* **2004**, *53* (4), 349–56.

(22) Robey, R. W.; Honjo, Y.; Morisaki, K.; Nadjem, T. A.; Runge, S.; Risbood, M.; Poruchynsky, M. S.; Bates, S. E. Mutations at amino-acid 482 in the ABCG2 gene affect substrate and antagonist specificity. *Br. J. Cancer* **2003**, *89* (10), 1971–8.

(23) Robey, R. W.; Shukla, S.; Finley, E. M.; Oldham, R. K.; Barnett, D.; Ambudkar, S. V.; Fojo, T.; Bates, S. E. Inhibition of P-glycoprotein (ABCB1)- and multidrug resistance-associated protein 1 (ABCC1)-mediated transport by the orally administered inhibitor, CBT-1((R)). *Biochem. Pharmacol.* **2008**, *75* (6), 1302–12.

(24) Fu, L. W.; Zhang, Y. M.; Liang, Y. J.; Yang, X. P.; Pan, Q. C. The multidrug resistance of tumour cells was reversed by tetrandrine in vitro and in xenografts derived from human breast adenocarcinoma MCF-7/adr cells. *Eur. J. Cancer* **2002**, *38* (3), 418–26.

(25) Shi, Z.; Liang, Y. J.; Chen, Z. S.; Wang, X. W.; Wang, X. H.; Ding, Y.; Chen, L. M.; Yang, X. P.; Fu, L. W. Reversal of MDR1/P-glycoprotein-mediated multidrug resistance by vector-based RNA interference in vitro and in vivo. *Cancer Biol. Ther.* **2006**, *5* (1), 39–47.

(26) Rabindran, S. K.; Ross, D. D.; Doyle, L. A.; Yang, W.; Greenberger, L. M. Fumitremorgin C reverses multidrug resistance in cells transfected with the breast cancer resistance protein. *Cancer Res.* **2000**, *60* (1), 47–50.

(27) Yan, Y. Y.; Zheng, L. S.; Zhang, X.; Chen, L. K.; Singh, S.; Wang, F.; Zhang, J. Y.; Liang, Y. J.; Dai, C. L.; Gu, L. Q.; Zeng, M. S.; Talele,

- T. T.; Chen, Z. S.; Fu, L. W. Blockade of Her2/neu binding to Hsp90 by emodin azide methyl anthraquinone derivative induces proteasomal degradation of Her2/neu. *Mol. Pharmaceutics* **2011**, *8* (5), 1687–97.
- (28) Xiang, Q. F.; Wang, F.; Su, X. D.; Liang, Y. J.; Zheng, L. S.; Mi, Y. J.; Chen, W. Q.; Fu, L. W. Effect of BIBF 1120 on reversal of ABCB1-mediated multidrug resistance. *Cell. Oncol. (Dordrecht)* **2011**, *34* (1), 33–44.
- (29) Guo, B. H.; Feng, Y.; Zhang, R.; Xu, L. H.; Li, M. Z.; Kung, H. F.; Song, L. B.; Zeng, M. S. Bmi-1 promotes invasion and metastasis, and its elevated expression is correlated with an advanced stage of breast cancer. *Mol. Cancer* **2011**, *10* (1), 10.
- (30) Bayram, H.; Ito, K.; Issa, R.; Ito, M.; Sukkar, M.; Chung, K. F. Regulation of human lung epithelial cell numbers by diesel exhaust particles. *Eur. Respir. J.* **2006**, *27* (4), 705–13.
- (31) Lee, S. Y.; Jeon, D. G.; Cho, W. H.; Song, W. S.; Kim, M. B.; Park, J. H. Preliminary study of chemosensitivity tests in osteosarcoma using a histoculture drug response assay. *Anticancer Res.* **2006**, *26* (4B), 2929–32.
- (32) Chen, Z.; Gu, J. Immunoglobulin G expression in carcinomas and cancer cell lines. *FASEB J.* **2007**, *21* (11), 2931–8.
- (33) Sung, J. M.; Cho, H. J.; Yi, H.; Lee, C. H.; Kim, H. S.; Kim, D. K.; Abd El-Aty, A. M.; Kim, J. S.; Landowski, C. P.; Hediger, M. A.; Shin, H. C. Characterization of a stem cell population in lung cancer A549 cells. *Biochem. Biophys. Res. Commun.* **2008**, *371* (1), 163–7.
- (34) Mi, Y. J.; Liang, Y. J.; Huang, H. B.; Zhao, H. Y.; Wu, C. P.; Wang, F.; Tao, L. Y.; Zhang, C. Z.; Dai, C. L.; Tiwari, A. K.; Ma, X. X.; To, K. K.; Ambudkar, S. V.; Chen, Z. S.; Fu, L. W. Apatinib (YN968D1) reverses multidrug resistance by inhibiting the efflux function of multiple ATP-binding cassette transporters. *Cancer Res.* **2010**, *70* (20), 7981–91.
- (35) Aller, S. G.; Yu, J.; Ward, A.; Weng, Y.; Chittaboina, S.; Zhuo, R.; Harrell, P. M.; Trinh, Y. T.; Zhang, Q.; Urbatsch, I. L.; Chang, G. Structure of P-glycoprotein reveals a molecular basis for poly-specific drug binding. *Science* **2009**, *323* (5922), 1718–22.
- (36) Shi, Z.; Tiwari, A. K.; Shukla, S.; Robey, R. W.; Singh, S.; Kim, I. W.; Bates, S. E.; Peng, X.; Abraham, I.; Ambudkar, S. V.; Talele, T. T.; Fu, L. W.; Chen, Z. S. Sildenafil reverses ABCB1- and ABCG2-mediated chemotherapeutic drug resistance. *Cancer Res.* **2011**, *71* (8), 3029–41.
- (37) Ambudkar, S. V.; Dey, S.; Hrycyna, C. A.; Ramachandra, M.; Pastan, I.; Gottesman, M. M. Biochemical, cellular, and pharmacological aspects of the multidrug transporter. *Annu. Rev. Pharmacol. Toxicol.* **1999**, *39*, 361–98.
- (38) Petrasch, S.; Welt, A.; Reinacher, A.; Graeven, U.; Konig, M.; Schmiegel, W. Chemotherapy with cisplatin and paclitaxel in patients with locally advanced, recurrent or metastatic oesophageal cancer. *Br. J. Cancer* **1998**, *78* (4), 511–4.
- (39) Donnenberg, V. S.; Donnenberg, A. D. Multiple drug resistance in cancer revisited: the cancer stem cell hypothesis. *J. Clin. Pharmacol.* **2005**, *45* (8), 872–7.
- (40) Zhou, S.; Schuetz, J. D.; Bunting, K. D.; Colapietro, A. M.; Sampath, J.; Morris, J. J.; Lagutina, I.; Grosveld, G. C.; Osawa, M.; Nakauchi, H.; Sorrentino, B. P. The ABC transporter Bcrp1/ABCG2 is expressed in a wide variety of stem cells and is a molecular determinant of the side-population phenotype. *Nat. Med.* **2001**, *7* (9), 1028–34.
- (41) Rosenberg, M. F.; Velarde, G.; Ford, R. C.; Martin, C.; Berridge, G.; Kerr, I. D.; Callaghan, R.; Schmidlin, A.; Wooding, C.; Linton, K. J.; Higgins, C. F. Repacking of the transmembrane domains of P-glycoprotein during the transport ATPase cycle. *EMBO J.* **2001**, *20* (20), 5615–25.
- (42) Shi, Z.; Peng, X. X.; Kim, I. W.; Shukla, S.; Si, Q. S.; Robey, R. W.; Bates, S. E.; Shen, T.; Ashby, C. R., Jr.; Fu, L. W.; Ambudkar, S. V.; Chen, Z. S. Erlotinib (Tarceva, OSI-774) antagonizes ATP-binding cassette subfamily B member 1 and ATP-binding cassette subfamily G member 2-mediated drug resistance. *Cancer Res.* **2007**, *67* (22), 11012–20.
- (43) Demel, M. A.; Kramer, O.; Etmayer, P.; Haakma, E. E.; Ecker, G. F. Predicting ligand interactions with ABC transporters in ADME. *Chem. Biodiversity* **2009**, *6* (11), 1960–9.
- (44) Klopman, G.; Shi, L. M.; Ramu, A. Quantitative structure-activity relationship of multidrug resistance reversal agents. *Mol. Pharmacol.* **1997**, *52* (2), 323–34.
- (45) Crivori, P.; Reinach, B.; Pezzetta, D.; Poggesi, I. Computational models for identifying potential P-glycoprotein substrates and inhibitors. *Mol. Pharmaceutics* **2006**, *3* (1), 33–44.
- (46) Pajeva, I. K.; Globisch, C.; Wiese, M. Combined pharmacophore modeling, docking, and 3D QSAR studies of ABCB1 and ABCG1 transporter inhibitors. *ChemMedChem* **2009**, *4* (11), 1883–96.
- (47) Bavetsias, V.; Large, J. M.; Sun, C.; Bouloc, N.; Kosmopoulou, M.; Matteucci, M.; Wilsher, N. E.; Martins, V.; Reynisson, J.; Atrash, B.; Faisal, A.; Urban, F.; Valenti, M.; de Haven Brandon, A.; Box, G.; Raynaud, F. I.; Workman, P.; Eccles, S. A.; Bayliss, R.; Blagg, J.; Linardopoulos, S.; McDonald, E. Imidazo[4,5-b]pyridine derivatives as inhibitors of Aurora kinases: lead optimization studies toward the identification of an orally bioavailable preclinical development candidate. *J. Med. Chem.* **2010**, *53* (14), 5213–28.
- (48) Bavetsias, V.; Sun, C.; Bouloc, N.; Reynisson, J.; Workman, P.; Linardopoulos, S.; McDonald, E. Hit generation and exploration: imidazo[4,5-b]pyridine derivatives as inhibitors of Aurora kinases. *Bioorg. Med. Chem. Lett.* **2007**, *17* (23), 6567–71.